

# DENSITY PROFILES OF DARK HALOS FROM THEIR MASS ACCRETION HISTORIES

M. A. Alvarez,<sup>1,2</sup> K. Ahn,<sup>1</sup> and P. R. Shapiro<sup>1</sup>

## RESUMEN

**El resumen será traducido al español por los editores.** We use the universal mass accretion history recently reported for simulations of halo formation in the cold dark matter model (CDM) to analyze the formation and growth of a single halo. We derive the time-dependent density profile three different ways, based upon three approximations of successively greater realism: equilibrium, radial orbits, and a fluid approximation. For the equilibrium model, the density profile is well-fit by either an NFW or Moore profile over a limited range of radii and scale factors. For the radial orbit model, we find profiles which are generally steeper than the NFW profile, with an inner logarithmic slope approaching -2, consistent with a purely radial collisionless system. In the fluid approximation, we find good agreement with the NFW and Moore profiles for radii resolved by N-body simulations ( $r/r_{200} \geq 0.01$ ), and an evolution of concentration parameter nearly identical to that found in N-body simulations. The evolving structure of cosmological halos is therefore best understood as the effect of a time-varying rate of mass infall on a smoothly distributed, isotropic, collisionless fluid.

## ABSTRACT

We use the universal mass accretion history recently reported for simulations of halo formation in the cold dark matter model (CDM) to analyze the formation and growth of a single halo. We derive the time-dependent density profile three different ways, based upon three approximations of successively greater realism: equilibrium, radial orbits, and a fluid approximation. For the equilibrium model, the density profile is well-fit by either an NFW or Moore profile over a limited range of radii and scale factors. For the radial orbit model, we find profiles which are generally steeper than the NFW profile, with an inner logarithmic slope approaching -2, consistent with a purely radial collisionless system. In the fluid approximation, we find good agreement with the NFW and Moore profiles for radii resolved by N-body simulations ( $r/r_{200} \geq 0.01$ ), and an evolution of concentration parameter nearly identical to that found in N-body simulations. The evolving structure of cosmological halos is therefore best understood as the effect of a time-varying rate of mass infall on a smoothly distributed, isotropic, collisionless fluid.

*Key Words:* **COSMOLOGY: THEORY — DARK MATTER — GALAXIES: FORMATION — GALAXIES: KINEMATICS AND DYNAMICS — LARGE-SCALE STRUCTURE OF UNIVERSE**

## 1. INTRODUCTION

Current understanding of dark matter halos relies upon N-body simulations of collisionless cold dark matter (CDM) with Gaussian-random-noise initial conditions. Two “universal” profiles bracket the results; (Navarro, Frenk, & White 1997; Moore et al. 1998). The NFW(Moore) profile has an inner density profile  $\rho \propto r^{-1}(r^{-1.5})$ . Wechsler et al. (2002) (WBPkd hereafter) found that the mass and concentration of individual N-body CDM halos grow over time according to simple universal formulae. In what follows, we attempt to explain this result.

## 2. THREE DIFFERENT MODELS

We attempt to understand the form and evolution of dark matter halos with three spherically-symmetric models; equilibrium, radial orbits, and an isotropic fluid. Each model assumes that the mass  $M_{\text{vir}}$  within an overdensity  $\delta_{\text{vir}}$  follows the relation given by WBPkd

$$M_{\text{vir}}(a) = M_{\infty} \exp[-Sa_c/a], \quad (1)$$

where  $a_c$  is the scale factor at collapse and  $S$  is the logarithmic mass accretion rate  $d(\ln M_{\text{vir}})/d(\ln a)$  when  $a = a_c$ . Such a relation is claimed to be a good fit to the evolution of halos of different masses and formation epochs. As in WBPkd, we have chosen  $S = 2$  and  $\delta_{\text{vir}} = 200$ , so that the halo has a mass  $M_{200}$  and radius  $r_{200}$ . We have found an initial per-

<sup>1</sup>Department of Astronomy, University of Texas at Austin, Austin, TX 78712

<sup>2</sup>DOE Computational Science Graduate Fellow

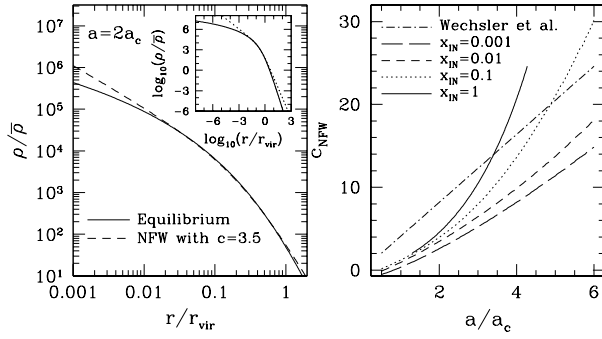


Fig. 1. (Left) Density profile from equilibrium model along with best-fitting NFW profile for this profile at present. Inset in upper-right shows same over much larger range. (Right) Evolution of NFW concentration parameter in the equilibrium model. Different line types indicate different ranges  $x_{\text{in}} < x < 1$ , within which halo was fit to an NFW profile, where  $x \equiv r/r_{\text{vir}}, r_{\text{vir}} \equiv r_{200}$ .

turbation profile consistent with equation (1),

$$\frac{\delta M}{M} \equiv \frac{M - \bar{M}}{\bar{M}} = \delta_i \ln \left[ \frac{M}{bM_\infty} \right], \quad (2)$$

where  $\delta_i$  depends on the initial scale factor  $a_i$  and  $\delta_{\text{vir}}$ , and  $\bar{M}$  is the unperturbed mass. The free parameter  $b$  is unity in the absence of pressure or shell crossing inside of  $r_{\text{vir}}$ .

### 2.1. Equilibrium

In the simplest model, we have made the assumption of complete equilibrium inside the halo, so that the velocity is zero for  $r < r_{\text{vir}} \equiv r_{200}$ . The mass of

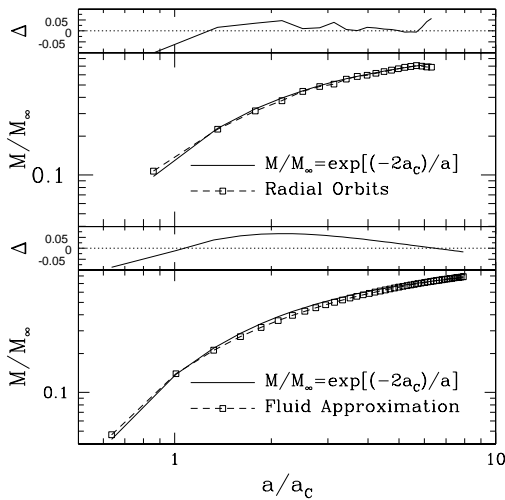


Fig. 2. Evolution of mass for the radial orbits (top) and fluid approximation (bottom) simulations. Shown above each are the fractional deviations  $\Delta \equiv (M_{\text{exact}} - M)/M$ .

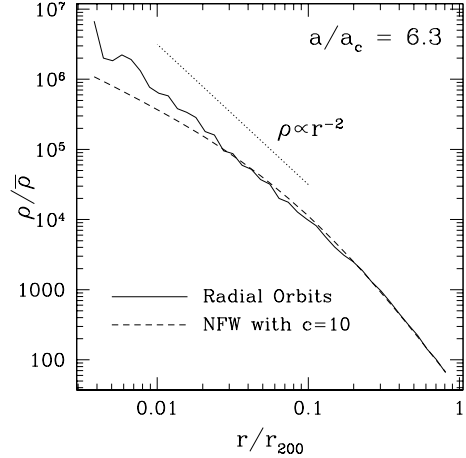


Fig. 3. Density profile at the end of the radial orbit simulation.

the halo is given by

$$M_{\text{vir}}(a) = \frac{4\pi}{3} \delta_{\text{vir}} \bar{\rho} r_{\text{vir}}^3, \quad (3)$$

where  $\bar{\rho}$  is the mean density at that epoch. Mass continuity implies the density  $\rho_{\text{vir}}$  just inside the virial radius is

$$\frac{dM_{\text{vir}}}{da} = 4\pi \rho_{\text{vir}} r_{\text{vir}}^2 \frac{dr_{\text{vir}}}{da}. \quad (4)$$

Differentiating equation (3) and combining with equations (1) and (4) yields

$$\frac{\rho_{\text{vir}}}{\rho_0} = \delta_{\text{vir}} a^{-3} \left[ 1 + \frac{3a}{S a_c} \right]^{-1}, \quad (5)$$

where  $\rho_0$  is the mean background density at  $a = 1$ . The virial radius is given by

$$\frac{r_{\text{vir}}}{r_0} = a \exp \left[ \frac{-S a_c}{3} \left( \frac{1}{a} - 1 \right) \right]. \quad (6)$$

Equations (5) and (6) are parametric in  $a$ , implying a radial density profile  $\rho(r) = \rho_{\text{vir}}(r_{\text{vir}})$  which is frozen in place as matter crosses  $r_{\text{vir}}$ . Taking the limit in which  $a \rightarrow \infty$ , the outer density profile approaches  $\rho \propto r^{-4}$  at late times, consistent with finite mass, while the inner slope becomes asymptotically flat. The NFW profile is given by

$$\frac{\rho(x)}{\bar{\rho}} = \frac{\delta_{\text{vir}} g(c)}{3x(1+cx)^2}, \quad (7)$$

where

$$g(c) = \frac{c^2}{\ln(1+c) - c/(1+c)}, \quad (8)$$

and  $x \equiv r/r_{\text{vir}}$ . Combining equations (5) and (7) with  $x = 1$ , yields an equation for the evolution of

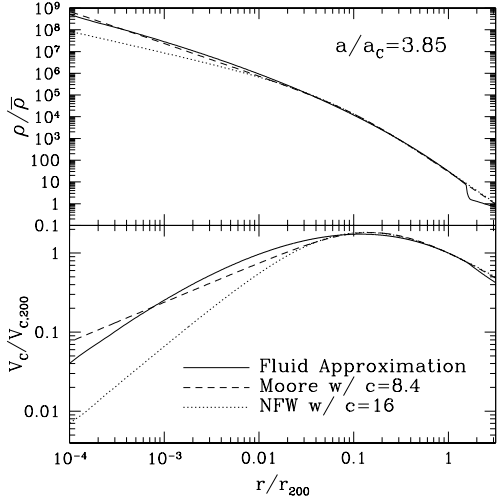


Fig. 4. (Top) Density profile at the end of the isotropic fluid calculation. (Bottom) Circular velocity profile.

concentration with scale factor (see Fig. 1),

$$\frac{a}{a_c} = S \left[ \frac{(1+c)^2}{g(c)} - \frac{1}{3} \right]. \quad (9)$$

### 2.2. Radial Orbits

We use a finite-difference spherical mass shell code to follow the evolution of a small amplitude perturbation which is chosen so that the resulting virial mass will evolve according to equation (1) from an initial perturbation given by equation (2). The shell code has an inner reflecting core and the results presented here used 20,000 shells (see Figs. 2 and 3).

### 2.3. Fluid Approximation

The collisionless Boltzmann equation in spherical symmetry yields fluid conservation equations ( $\gamma = 5/3$ ) when random motions are isotropic. Halos in N-body simulations have radially biased random motion, but the bias is small, especially in the center. This model is therefore a better approximation to halo formation in N-body simulations than one with purely radial motion. We use a 1-D, spherical, Lagrangian hydrodynamics code as in Thoul & Weinberg (1995), using 1,000 zones logarithmically spaced in mass (see Figs. 2, 4, and 5). The initial conditions were chosen in the same way as those for the radial orbit model (Eq. 2), with zero initial temperature.

## 3. RESULTS

- Equilibrium model does not reproduce linear evolution of concentration parameter with scale factor reported by WPKD, but can be fit by

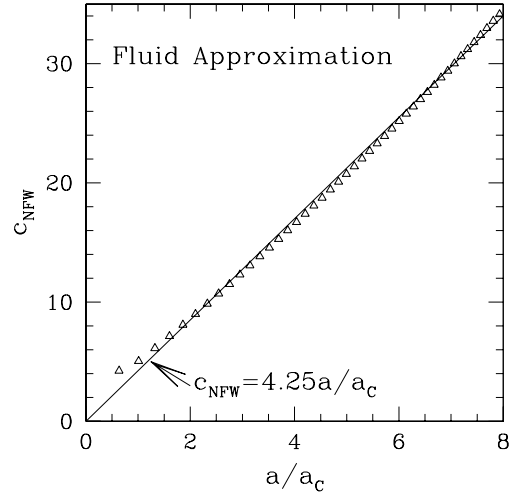


Fig. 5. Evolution of concentration parameter with scale factor in the isotropic fluid calculation.

an NFW profile over a limited range of radii and scale factors (Fig. 1).

- Mass evolution for a perturbation given by equation (2) is close to that of equation (1) (Fig. 2).
- The radial orbit model fails to reproduce the inner slope of the NFW profile, approaching  $\rho \propto r^{-2}$  instead, consistent with the argument of Richstone & Tremaine (1984) (Fig. 3).
- Fluid approximation halo is well-fitted by NFW and Moore profiles for radii resolved by N-body simulations ( $r/r_{200} \geq 0.01$ ) (Fig. 4).
- Evolution of NFW concentration parameter in the fluid approximation is a close match to that of WPKD, with  $c_{\text{NFW}} = 4.25a/a_c$  a good fit (Fig. 5). WPKD reported  $c_{\text{NFW}} = 4.1a/a_c$ . Complicated merging process is not necessary in order to understand density profile evolution.

This work was supported in part by grants NASA ATP NAG5-10825 and NAG5-10826 and Texas Advanced Research Program 3658-0624-1999.

## REFERENCES

- Moore, B., Governato, F., Quinn, T., Stadel, J., & Lake, G. 1998, ApJ, 499, L5
- Navarro, J.F., Frenk, C.S., & White S.D.M. 1997, ApJ, 490, 493
- Richstone, D.O. & Tremaine, S. 1984, ApJ, 286, 27
- Thoul, A. A. & Weinberg, D.H. 1995, ApJ, 442, 480
- Wechsler R.H., Bullock, J.S., Primack, J.R., Kravtsov, A.V., & Dekel, A. 2002, ApJ, 568, 52